Title
The energy level alignment at metal–molecule interfaces using Wannier–Koopmans method

Journal
Applied Physics Letters, 108(26)

ISSN
0003-6951

Authors
Ma, Jie
Liu, Zhen-Fei
Neaton, Jeffrey B
et al.

Publication Date
2016-06-27

DOI
10.1063/1.4955128

Peer reviewed

Energy level alignment at metal-molecule interfaces using Wannier-Koopmans method

Jie Ma,[1,2] Zhen-Fei Liu,[1,3] Jeffrey B. Neaton,[1,3] and Lin-Wang Wang[1,*]

[1] *Materials Sciences Division, Lawrence Berkeley National Laboratory, Berkeley, California 94720, USA*

[2] *Joint Center for Artificial Photosynthesis, Lawrence Berkeley National Laboratory, Berkeley, California 94720, USA*

[3] *Department of Physics, University of California, Berkeley, California, 94720, USA*

(Dated: May 13, 2016)

Abstract

We apply a newly developed Wannier-Koopmans method (WKM), based on density functional theory (DFT), to calculate the electronic energy level alignment at an interface between a molecule and metal substrate. We consider two systems: benzenediamine on Au (111), and a bipyridine-Au molecular junction. The WKM calculated level alignment agrees well with the experimental measurements where available, as well as previous *GW* and DFT+Σ results. Our results suggest that the WKM is a general approach that can be used to correct DFT eigenvalue errors, not only in bulk semiconductors and isolated molecules, but also hybrid interfaces.

* lwwang@lbl.gov

Many physical processes in nanoscience that impact device function take place at the interfaces between molecules and metal electrodes [1], such as charge transfer in organic solar cells[2], charge transport across molecular junctions[3], and chemical reactions relevant to photocatalysis such as water splitting[4]. Underlying the mechanisms of these dynamical processes is interfacial electronic energy level alignment: the difference between a frontier molecular orbital energy and the Fermi level of the metal electrode. Energy level alignment is related to the barrier for charge transfer across the interface and therefore can dictate efficiency of the dynamical processes mentioned above. An accurate description and calculation of level alignment at interfaces is thus crucial for understanding, controlling, and predicting dynamical properties at the interfaces.

Complementary to experimental techniques such as photoemission spectroscopy (PES)[5], first-principles electronic structure calculations have provided critical understanding of the level alignment based on the quasiparticle energies of molecules in chemical contact with metal electrodes. The systems involved in molecule-metal interface modeling usually consist of hundreds of atoms. Due to the complexity of such systems, density functional theory (DFT) [6, 7] is often used as the starting point in approaching this problem. Although DFT with common approximate exchange-correlation functionals can in general be accurate for total energy related properties such as geometries and forces, there is no fundamental theorem in DFT that guarantees the validity of Kohn-Sham (KS) eigenvalues as quasiparticle energies [8], at least other than the highest occupied KS eigenvalue. In practice, with local or semi-local functionals, KS eigenvalues can differ from quasiparticle energies by a few eV's, leading to significant errors in gaps of semiconductors and level alignment at interfaces. Many-body perturbation theory (MBPT) within the GW approximation [9, 10] (G stands for the Green's function, W for the screened Coulomb interaction) is a formally rigorous way to compute quasiparticle energies and level alignment. However due to its high computational cost, it is still not often used in routine calculations. Simplified model GW approaches [11], such as DFT+Σ [12–14], are applicable for weakly interacting interfaces in specific limits, which allows the treatment of metal substrate and molecule separately. However, a more unified theoretical tool that, at a reasonable computational cost, is accurate for both band gaps of bulk semiconductors and level alignments of complex systems, is desirable, and would have a broad range of applications.

In this work, we generalize a recently developed computational approach[15], based on

DFT, to calculate electronic energy level alignment at the interfaces. This method (the Wannier-Koopmans method, WKM) uses Wannier functions to enforce compliance with the generalized Koopmans' theorem [16]. Our previous study [15] has already demonstrated the prediction of accurate band gaps of common semiconductors, as well as charged excitations of gas-phase molecules. However, as these are single component systems, it remains to be seen whether the same approach can work for heterogenous systems, especially for the level alignment between constituents at an interface. Organic molecules adsorbed on a metal substrate is an extreme example of such a heterostructure.

Here, we examine the WKM method for two prototypical metal-molecule interfaces: (a) benzenediamine (BDA) adsorbed on Au(111) surface, and (b) a bipyridine(BP)-Au junction. System (a) has been well studied by experiment [17], *GW* [18], and DFT+Σ [18, 19]; and system (b) has been studied in the context of charge transport through molecular junctions [20–22], with both break-junction experiments and DFT+Σ. The atomic geometries [23] of these two systems are first optimized using DFT with the Perdew-Burke-Ernzerhof (PBE) functional [24] as implemented in SIESTA [25], shown in Fig. 1. In system (a), the BDA molecule is resting flat on a Au(111) substrate, thus the interaction between the molecule and the Au(111) surface is extremely short-ranged. The energy level associated with the highest occupied molecular orbital (HOMO) is deep inside the valence band of the Au (e.g., the HOMO energy is much lower than the Au Fermi energy, E_F). Photoemission spectroscopy [17] has been used to measure the HOMO resonance energy relative to the Au Fermi level. Prior *GW* calculations[18] have obtained results similar to the experiments. On the other hand, DFT calculations using the PBE functional yield resonance energies about 1.5 eV different from the experiments. We also note that very recently, Ref. [19] reported a linear chain phase for the BDA molecules on the Au(111) surface, which is energetically favored compared to the geometry studied in Ref. [18] and this work. However, as it is of primary interest in this work to compare the performance of the WKM method with other methods such as DFT+Σ and *GW* for this system, we adopt the same geometry here as in Ref. [18]. In system (b), a BP molecule is interfaced on both sides by Au electrodes, as in a single-molecule break-junction experiment. Using a DFT+Σ calculation as in previous work [20, 21], corroborated by experiments [22], predicted that the lowest unoccupied molecular orbital (LUMO) energy of BP is about 1.5 eV above the Au electrode Fermi level. The above two systems allow us to examine two different molecule-metal environments: the first

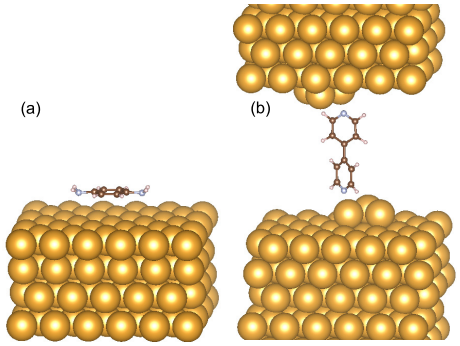

FIG. 1. Geometries of the two prototypical interface systems studied in this work: (a) BDA adsorbed on Au(111) surface; and (b) BP-Au junction.

consists of only one surface and features a HOMO resonance near E_F, while the second is a junction and features a LUMO resonance near E_F. In addition, in the first system, the molecule is adsorbed flat on the surface, while in the second system, the molecule is bound on either side to a motif consisting of a Au trimer.

In the WKM, the total energy of the system is expressed as:

$$E = E_{\rm PBE} + \sum_l \tilde{E}_l(s_l)\,,\ s_l \in [0,1], \tag{1}$$

with $E_{\rm PBE}$ being the total energy of the system calculated from conventional DFT (using PBE [24] in this work), and $\tilde{E}_l(s_l) = [E_l(N \pm 1) - E(N)] \times s_l - [E_l(N \pm s_l) - E(N)]$ ("+" for adding electrons to an unoccupied Wannier orbital ϕ_l, and "−" for removing electrons from an occupied Wannier orbital ϕ_l). $E_l(N \pm s_l)$ is the total energy calculated from PBE after adding/removing s_l electrons associated with the ϕ_l orbital. Note: $s_l = \sum_i |\langle\phi_l|\psi_i\rangle|^2 f_i$, where the ψ_i is the KS orbital with occupation number f_i. Thus, minimizing E with respect to ψ_i, we obtain a modified KS equation

$$\left\{ H_{\rm PBE} + \sum_l \lambda_l |\phi_l\rangle\langle\phi_l| \right\} |\psi_i\rangle = \epsilon_i |\psi_i\rangle, \tag{2}$$

with $\lambda_l = \partial\tilde{E}_l(s_l)/\partial s_l|_{s_l=0}$, the magnitude of the corrections to the KS eigenvalues.

In the above equations, the $\{\phi_l\}$ are Wannier functions constructed from the occupied and unoccupied subspaces of the molecule. The modified KS equation provides eigenvalues

which can better approximate quasiparticle energies. The above procedure differs from the commonly used ΔSCF method in that it employs Wannier functions ϕ_l, instead of the KS eigenstates.

One major step in the WKM is to calculate λ_l, which is obtained from $\tilde{E}_l(s_l)$, the total energy of the system when ϕ_l is occupied with s_l electrons. For each l, a special self-consistent field (SCF) algorithm is used to calculate $\tilde{E}_l(s_l)$ for a given s_l, much like in the calculation of the usual ground state energy. However, in this special SCF procedure, the density is expressed as:

$$\rho(\mathbf{r}) = \alpha_l |\phi_l(\mathbf{r})|^2 + \sum_j |\varphi_j(\mathbf{r})|^2, \tag{3}$$

where for l in the valence band, $\alpha_l = 1 - s_l$ and for l in the conduction band, $\alpha_l = s_l$. The sum over j is for all fully occupied orbitals φ_j, i.e., $N-1$ for l in the valence band and N for l in the conduction band. Notice that φ_j is only used in the calculation of $\tilde{E}_l(s_l)$ and is not to be confused with ψ_i in Eq. (2). For technical details, please see Ref. [15]. In this special SCF procedure, for each l, we keep ϕ_l fixed and enforce $\langle \phi_l | \varphi_j \rangle = 0$, allowing φ_j to change variationally to minimize $E_l(N \pm s_l)$. Our SCF calculation captures the screening effects of all the other electrons on the s_l fractional charge in the l-th Wannier orbital. Besides the ground-state energy, for each Wannier function ϕ_l, typically two such special SCF calculations are needed to compute $\tilde{E}_l(s_l)$ in order to get λ_l: one with $s_l = 0$ ($s_l = 1$) for occupied (unoccupied) Wannier function ϕ_l, and one for s_l greater than but close to 0 (smaller than but close to 1).

The Wannier functions on the molecules are constructed using the Wannier90 [26] package with the atomic orbital projection method. One of such constructed occupied Wannier functions for system (a) [Fig. 1(a)] and an unoccupied Wannier function for system (b) [Fig. 1(b)] are shown in Fig. 2(a) and (b), respectively. For the Wannier function shown in Fig. 2(a), it contributes most to BDA HOMO, i.e., $|\langle \phi_l | \psi_{\mathrm{HOMO}} \rangle|^2$ is largest (=0.274) among all $\{\phi_l\}$. For the Wannier function shown in Fig. 2(b), it contributes most to BP LUMO, $|\langle \phi_l | \psi_{\mathrm{LUMO}} \rangle|^2 = 0.396$, more than all the other Wannier functions in the calculation.

Our SCF calculations are performed in a supercell with periodic boundary conditions. Such SCF calculations are similar to a defect total energy calculation with charged or uncharged defect states (here the defect state is the Wannier orbital), and thus techniques [27] to correct the artificial image charge interactions due to the finite size of the supercell can

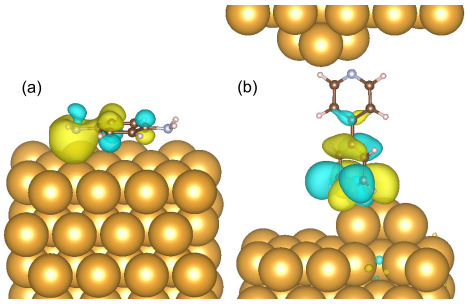

FIG. 2. (a) The occupied Wannier function for the BDA molecule adsorbed on Au(111) that contributes most to BDA HOMO. (b) The unoccupied Wannier function for the BP molecule in the junction that contributes most to BP LUMO. For details, see text.

be applied here. When we remove a partial electron from the Wannier function in Fig. 2(a), or add a partial electron in the Wannier function in Fig. 2(b), the supercell is no longer charge neutral, and the image-image interaction of the extra charge due to the finite size of the supercell becomes significant. However, we note that in a semi-infinite system, the extra s_l charge on the molecule will be completely compensated by the metal surface charge of opposite sign and a dipole is formed near the surface [28]. In practice, we mimic this situation in our calculation using a *finite* Au slab. We use overall neutral systems, but subtract the dipole-dipole image interaction energy from the total energy $\tilde{E}_l(s_l)$. We calculate the dipole moment along the z-axis of the system as $d = \int z\Delta\rho(r)d^3r$, here $\Delta\rho(r)$ is the SCF charge density change due to the placing (or removing) of the s_l electron on the Wannier orbital. The dipole-dipole image interaction energy is then calculated as $2\sum_i d^2/|\mathbf{R}_i - \mathbf{R}_0|^3$, where $|\mathbf{R}_i - \mathbf{R}_0|$ is the distance between neighboring images and the factor of 2 appears since the charge in the metal can be approximated as a delocalized surface charge, instead of a localized point charge. After these corrections, for BDA in Fig. 1(a), the dipole-dipole image correction is about 0.2 eV, and for BP in Fig. 1(b), the dipole correction is negligible due to the symmetry of the system.

Having performed total energy calculations for $\tilde{E}_l(s_l)$, we then calculate λ_l for the Wannier functions. For example, the λ_l for the Wannier function of BDA shown in Fig. 2(a) is 2.1 eV, while the λ_l for the Wannier function of BP shown in Fig. 2(b) is 0.64 eV. We then

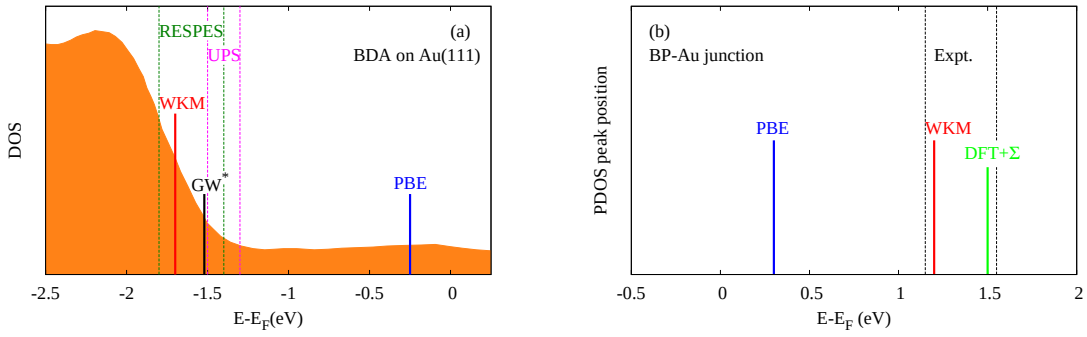

FIG. 3. (a) Projected density of states for BDA adsorbed on Au(111) surface. Experimental results from RESPES and UPS are shown as a range between two vertical lines. Theoretical results from PBE, *GW**, and WKM are shown. WKM result is from this work, and all others are taken from Ref. [18]. Orange shaded region shows the density of states of Au. (b) Projected density of states (PDOS) peaks for BP in a junction. Experimental estimation is shown as a range between two vertical lines, Results from DFT+Σ, PBE, and WKM are shown. WKM result is from this work, and all others are taken from Refs. [20, 22].

solve Eq. (2) for the corrected eigenvalues for the molecules. Note, we have not included the λ_l term in Eq. (2) for states in the Au electrode. This is because the Au pseudopotential in this study has been carefully tuned to yield the correct work function for Au(111) surface [29], thus a PBE calculation will yield the correct Au Fermi energy.

The results of our calculation are shown in Fig. 3. For BDA, the PBE HOMO energy is at -0.25 eV below the Au Fermi energy as shown in Fig. 3(a). Ultraviolet photoelectron spectroscopy (UPS) measurements place this level at around -1.4 eV below Au Fermi energy, while the resonant photoelectron spectroscopy (RESPES) measurement indicates that the molecule level should be within the window of -1.8 to -1.4 eV as shown in Fig. 3(a) [18]. Thus, the PBE energy alignment is more than 1 eV away from the experimental result. The WKM HOMO level is at about -1.7 eV below the Au Fermi energy, within the range measured by RESPES. We note that there is always the geometry uncertainty when comparing calculations to experiments, and a recent work Ref. [19] found a more energetically favorable structure than the one used here, as discussed before. We also show additional theoretical results from Ref. [18] for comparison. After the *post hoc* correction (see Ref. [18]), the final

GW result [*GW** in Fig. 3(a)] is above 0.15 eV higher than the WKM result, also agrees well with the experiments. The advantage of the WKM compared to *GW** is its much lower computational cost.

For the case of BP, the PBE LUMO level is at 0.3 eV above the Au Fermi energy [Fig. 3(b)]. However, the transport measurements suggest [20, 22] that the LUMO level should be about 1.2-1.6 eV above the Au Fermi energy [Fig. 3(b)]. the WKM LUMO is at about 1.2 eV above the Au Fermi energy, in good agreement with experiments. We have also calculated the level alignment using our previous DFT+Σ method [12, 13] as applied in Refs. [20, 22]. The result is shown in Fig. 3(b). Compared to the DFT+Σ, the current WKM approach does not need the use of a classical image charge model for the surface polarization and therefore can be extended beyond flat geometries. The surface polarization is calculated self-consistently at the DFT level with fractional charges in a single step in the WKM.

Thus, in conclusion, we found that the WKM method works well for level alignment of both HOMO-dominated and LUMO-dominated metal-molecule interfaces, and also for both the case where the molecule is very close to a flat surface and the case where the molecule is bound to a trimer and forms a junction with two electrodes. Compared with our previous DFT+Σ approach, the WKM can treat dielectric screening effects more accurately (especially when the molecule is very close to the substrate), and compared with the *GW* method, it is much cheaper. We thus shows that, the WKM method not only works well for bulk semiconductor and isolated molecules, but is also successful in predicting energy level alignment of heterogeneous interfaces.

Acknowledgments

This work is supported by the U.S. Department of Energy, Director, Office of Science, Office of Basic Energy Sciences, Materials Sciences and Engineering Division, under Contract No. DE-AC02-05CH11231, through the Material Theory program [KC2301] in Lawrence Berkeley National Laboratory. This work is also supported by the Molecular Foundry through the U.S. Department of Energy, Office of Basic Energy Sciences under the same contract number. This work uses the resource of National Energy Research Scientific Com-

puting center (NERSC).

---

[1] N. Koch, N. Ueno, and A. T. S. Wee, eds., *The Molecule-Metal Interface* (Wiley-VCH, 2013).

[2] A. Hagfeldt, G. Boschloo, L. Sun, L. Kloo, and H. Pettersson, Chem. Rev. **110**, 6595 (2010).

[3] L. Venkataraman, J. E. Klare, C. Nuckolls, M. S. Hybertsen, and M. L. Steigerwald, Nature **442**, 904 (2006).

[4] A. Kudo and Y. Miseki, Chem. Soc. Rev. **38**, 253 (2009).

[5] N. Ueno and S. Kera, Prog. Surf. Sci. **83**, 490 (2008).

[6] P. Hohenberg and W. Kohn, Phys. Rev. **136**, B864 (1964).

[7] W. Kohn and L. J. Sham, Phys. Rev. **140**, A1133 (1965).

[8] L. Kronik and S. Kümmel, Top. Curr. Chem. **347**, 137 (2014).

[9] L. Hedin, Phys. Rev. **139**, A796 (1965).

[10] M. S. Hybertsen and S. G. Louie, Phys. Rev. B **34**, 5390 (1986).

[11] L.-W. Wang, J. Phys. Chem. B. **109**, 23330 (2005).

[12] J. B. Neaton, M. S. Hybertsen, and S. G. Louie, Phys. Rev. Lett. **97**, 216405 (2006).

[13] S. Y. Quek, L. Venkataraman, H. J. Choi, S. G. Louie, M. S. Hybertsen, and J. B. Neaton, Nano Lett. **7**, 3477 (2007).

[14] D. A. Egger, Z.-F. Liu, J. B. Neaton, and L. Kronik, Nano Lett. **15**, 2448 (2015).

[15] J. Ma and L.-W. Wang, Sci. Rep. **6**, 24924 (2016).

[16] C.-O. Almbladh and U. von Barth, Phys. Rev. B **31**, 3231 (1985).

[17] M. Dell'Angela, G. Kladnik, A. Cossaro, A. Verdini, M. Kamenetska, I. Tamblyn, S. Y. Quek, J. B. Neaton, D. Cvetko, A. Morgante, and L. Venkataraman, Nano Lett. **10**, 2470 (2010).

[18] I. Tamblyn, P. Darancet, S. Y. Quek, S. Bonev, and J. B. Neaton, Phys. Rev. B **84**, 201402 (2011).

[19] G. Li, T. Rangel, Z.-F. Liu, V. R. Cooper, and J. B. Neaton, Phys. Rev. B **93**, 125429 (2016).

[20] S. Y. Quek, M. Kamenetska, M. L. Steigerwald, H. J. Choi, S. G. Louie, M. S. Hybertsen, J. B. Neaton, and L. Venkataraman, Nature Nanotechnology **4**, 230 (2009).

[21] J. R. Widawsky, P. Darancet, J. B. Neaton, and L. Venkataraman, Nano Lett. **12**, 354 (2012).

[22] T. Kim, P. Darancet, J. R. Widawsky, M. Kotiuga, S. Y. Quek, J. B. Neaton, and L. Venkataraman, Nano Lett. **14**, 794 (2014).

[23] The BDA-Au(111) geometry is adopted from Ref. [18], and the BP-Au junction geometry is optimized until all forces are less than 0.04 eV/Å, in a similar fashion as Refs. [20–22]. ().

[24] J. P. Perdew, K. Burke, and M. Ernzerhof, Phys. Rev. Lett. **77**, 3865 (1996).

[25] J. M. Soler, E. Artacho, J. D. Gale, A. García, J. Junquera, P. Ordejón, and D. Sánchez-Portal, J. Phys.: Condens. Matter **14**, 2745 (2002).

[26] A. A. Mostofi, J. R. Yates, Y.-S. Lee, I. Souza, D. Vanderbilt, and N. Marzari, Comput. Phys. Commun. **178**, 685 (2008).

[27] S.-H. Wei, Comp. Mat. Sci **30**, 337 (2004).

[28] A. M. Souza, I. Rungger, C. D. Pemmaraju, U. Schwingenschloegl, and S. Sanvito, Phys. Rev. B **88**, 165112 (2013).

[29] The Au pseudopotential is adopted from Ref. [13] and yields a lattice constant 4.22Å and a work function 5.3 eV for Au(111). ().